Soft Matter

PAPER

Room temperature sphere-to-rod growth of Pluronic® P85 micelles induced by salicylic acid†

P. Parekh,[a] R. Ganguly,*[b] V. K. Aswal[c] and P. Bahadur[a]

The influence of salicylic acid (SA) on the aggregation characteristics of Pluronic® P85 has been studied in the aqueous medium by dynamic light scattering (DLS), small angle neutron scattering (SANS), steady-state fluorescence and rheological measurements. DLS studies suggest that SA, which is used in the treatment of various skin diseases, induces a room temperature growth of the P85 micelles. Steady-state fluorescence studies and cloud point measurements attribute this to the ability of SA to stay in micellar corona and consequently dehydrate the copolymer micelles by displacing water from the corona region. A large increase in the viscosity of the P85 solutions accompanying the observed micellar growth, and SANS and rheological studies reveal that the P85 micelles undergo a sphere-to-rod shape transition in the presence of SA. Pluronics® being biomedically important surfactants, the observed effects suggest that P85 could be considered as a suitable agent as a carrier of SA, as well as a viscosity modifier of the formulations of SA. The studies also show that the effectiveness of SA in causing the observed micellar dehydration increases with a decrease in pH, which suggests that the observed effects of SA on the P85 micelles arise due to the presence of the unionized form of the SA in the micellar corona region. Rheological studies show that unlike other Pluronic® worm like micellar systems, the viscoelastic behavior of the present system shows close conformity with the Maxwell law. Such difference in the behavior has been attributed to faster restructuring and breaking processes of the P85 micelles due to the high hydrophilic PEO group content (50%) of P85 molecules.

Introduction

The commercial PEO–PPO–PEO based triblock copolymers, called Pluronics®, have been subjected to extensive studies in the last few decades because of their rich phase behavior[1–11] and numerous industrial and biomedical applications.[12–23] These non-ionic surfactants are unique in showing a strong temperature dependence of their self-assembly characteristics in the aqueous medium due to the differential solubility characteristics of their constituent blocks.[8] They remain as unimers at low temperature but start forming core–shell micelles comprising hydrophobic PPO blocks as cores and heavily hydrated hydrophilic PEO blocks as shells (corona) at their characteristic temperature called the critical micellar temperature (CMT).[9–11] Above CMT, a progressive dehydration of these core–shell micelles with an increase in temperature results in an increase in the micellar aggregation number and core size.[9,24,25] Such micellar restructuring processes with increase in temperature often lead to a sphere-to-rod micellar shape change when the size of the core becomes equal to the length of the stretched PPO chain.[26] Some of these Pluronics® also show critical behavior due to the onset of inter-micellar attractive interaction and consequent formation of large micellar clusters on approaching the cloud point (CP) of their aqueous solutions.[27–29]

The aggregation characteristics of Pluronics® are modified quite significantly in the presence of different additives that have strong influence over their solubilization characteristics in water.[30–42] Substances that increase the hydrophobic character of these copolymer molecules favor micelle formation and growth by reducing the critical micellar concentration (CMC), CMT, and the sphere-to-rod transition temperature of the copolymer solutions. On the other hand, the substances that increase their hydrophilic character show exactly opposite effects that lead to the destabilization of micelles. Pluronics® are considered as suitable agents as carriers of hydrophobic drugs,[13–23] and as extracting agents for different hydrophobic substances.[41,42] Salicylic acid (SA) is an important drug for the treatment of various skin diseases like acne, psoriasis, and photoaging.[43–48] Since it is poorly soluble in water, its solubilization characteristics in the

[a]Department of Chemistry, Veer Narmad South Gujarat University, Surat-395007, India. E-mail: paresh7884@gmail.com; pbahadur2002@yahoo.com
[b]Chemistry Division, Bhabha Atomic Research Center, Mumbai-400085, India. E-mail: rajibg@barc.gov.in; rajugang@yahoo.co.in; Fax: +91-22-25505151; Tel: +91-22-25590286
[c]Solid State Physics Division, Bhabha Atomic Research Center, Mumbai-400085, India. E-mail: vkaswal@barc.gov.in
† Electronic supplementary information (ESI) available. See DOI: 10.1039/c2sm25517k

aqueous solutions of biocompatible Pluronics® will be worth studying. In view of this we have carried out detailed studies on the effect of solubilization of SA on the aggregation characteristics of a biomedically important copolymer Pluronic® P85 (ref. 21–23) in aqueous medium. We observed that the copolymer micelles undergo dehydration because of entrapment of SA in the micellar corona region, and subsequently are subjected to a sphere-to-rod shape transition. The consequent increase in the viscosity of the copolymer solutions could be of interest because of its possible application as a viscosity modifier of the SA formulations.[49,50]

Experimental

Materials and sample preparation

The triblock copolymer Pluronics® P85 was procured from BASF Corp. Parsippany, NJ, USA and was used as received. Salicylic acid (analytical grade) was purchased from E. Merck. The copolymer solutions were prepared by weighing required amounts of water and copolymer and keeping them in a refrigerator overnight in tightly closed glass vials.

Methods

Dynamic light scattering (DLS). DLS measurements of the solutions were performed using a Malvern 4800 Autosizer employing 7132 digital correlator. The light source was a He–Ne laser operated at 633 nm with a maximum output power of 15 mW. The average decay rate was obtained by analyzing the electric field autocorrelation function $g^1(\tau)$ vs. time data using a modified cumulants method.[51] This method overcomes the limitations of cumulants analysis to fit the autocorrelation function data of samples with large polydispersity.[52] The apparent equivalent hydrodynamic radii of the micelles were calculated using the Stokes–Einstein equation. Measurements were made at five different angles ranging from 50° to 130°. To determine whether the scatterers are diffusive in nature, the average decay rate (Γ) for the samples was plotted against q^2 (q being the magnitude of the scattering vector given by $[4\pi n^*\sin(\theta/2)]/\lambda$, where n is the refractive index of the solvent, λ is the wavelength of laser light and θ is the scattering angle).

Viscometry. The absolute viscosities of the solutions were measured in a temperature controlled water bath by using size 50, size 150 and size 300 calibrated cannon ubbelohde viscometers, with viscometer constants of 0.004065, 0.03925 and 0.2775 centi-stokes s^{-1} respectively.[53] The measured flow times of the solutions in seconds were multiplied by the viscometer constant to get the kinematic viscosity of the solutions in centi-stokes. The spread in the flow time was found to remain within ±5 s. These kinematic viscosities were then multiplied by the density of water (taken as 1 g cm^{-3}) to obtain the viscosity of the solutions in centi-poise. The relative viscosities of the solutions were then calculated by dividing the obtained viscosity values by the viscosity of water at the room temperature.

Steady state fluorescence. Steady-state fluorescence spectra were recorded using a Hitachi (Tokyo, Japan) model F-4010 spectrofluorometer. The recorded spectra were corrected for the wavelength dependent instrument responses by measuring the spectrum of quinine sulfate and comparing it with the reported standard spectrum. All the emission spectra were recorded at 30 °C. The fluorescence probe used for the present study is Coumarin-153 (C153). Its concentration in the P85 solution was maintained such that the probability of having more than one C153 molecule in a single micelle was very low.

Small angle neutron scattering (SANS). SANS measurements were carried out on the samples prepared in D$_2$O at the SANS facility at DHRUVA reactor, Trombay. The mean incident wavelength was 5.2 Å with $\Delta\lambda/\lambda = 15\%$. The scattering was measured in the scattering vector (q) range of 0.017 to 0.3 Å^{-1}. The measured SANS data were corrected for the background, the empty cell contributions and the transmission, and were placed on an absolute scale using standard protocols. Correction due to the instrumental smearing was taken into account throughout the data analysis.[54]

The differential scattering cross-section per unit volume (dΣ/dΩ) of monodisperse micelles can be written as[55,56]

$$d\Sigma/d\Omega = NF_{mic}(q)S(q) + B \qquad (1)$$

N is the number density of the micelles and B is a constant term that represents the incoherent background scattering mainly from the hydrogen atoms present in the sample. $F_{mic}(q)$ is the form factor characteristic of specific size and shape of the scatterers and $S(q)$ is the structure factor that accounts for the inter-particle interaction. The P85 micelles can be considered as core–shell particles with different scattering length densities of the core and the shell. The structure of these micelles is described using a model consisting of hydrated PEO chains (blocks) attached to the surface of the hydrophobic core comprising the PPO blocks.[55–57] The shell is described as consisting of non-interacting Gaussian polymer chains and these chains are assumed to be displaced from the core (else the mathematical approximations will not work as the chains overlap each other and the core), i.e. a mushroom polymer configuration is assumed. Non-penetration of the chains into the core region is mimicked by moving the center of mass of the chains by a distance R_g away from the surface of the core, where R_g is the radius of the gyration of the PEO blocks. The form factor of the micelles $F_{mic}(q)$ comprises four terms: the self-correlation of the core, the self-correlation of the chains, the cross term between the core and chains, and the cross term between different chains. The scattering length densities of D$_2$O and the shell are quite close because of the presence of considerable amount of D$_2$O in the shell. The core being hydrophobic, however, will have significantly different scattering properties compared to the shell due to widely different scattering length densities of hydrogen and deuterium. This model has been successfully used to fit the SANS data of aqueous micellar solutions of different Pluronics®. The form factors for spherical and ellipsoidal micelles were used as formulated by Pedersen.[55–57] The inter-particle structure factor $S(q)$ for the spherical block copolymer micelles is usually captured by the analytical solution of the Ornstein–Zernike equation with the Percus–Yevick approximation, employing hard sphere interaction.[58]

In the case of polydisperse micelles, eqn (1) can be written as

$$d\Sigma/d\Omega(q) = \int d\Sigma/d\Omega(q,R_c)f(R_c)dR_c + B \quad (2)$$

The polydispersity in the micellar size ($R = R_c$) has been accounted for by a Schultz distribution as given by the equation

$$f(R_c) = [(z + 1)/R_{cm}]^{z+1}R_c^z\exp[-(z + 1)/R_{cm})R_c][1/(\Gamma(z + 1)] \quad (3)$$

where R_{cm} is the mean value of the distribution and z is the width parameter. The polydispersity of this distribution is given by $\Delta R_c/R_{cm} = 1/(z + 1)^{1/2}$.

The analyses of the data were carried out by using R_c, R_g, R_{hs}, ϕ and Z as variables. These parameters were optimized by means of a nonlinear least-square fitting program in Fortran.[59]

Rheology. Rheological measurements were conducted using an Anton Parr Physica MCR101 rheometer in a double gap concentric cylinder geometry (DG 26.7) with a Peltier temperature control.

Results and discussions

The effect of SA on the aggregation characteristics of Pluronic® P85 can be understood from its influence on the cloud point (CP) or the phase separation temperature of its aqueous solutions. The variation of CP of 5% P85 solutions as a function of SA concentration is shown in Fig. 1a. The figure shows that the CP decreases progressively with increase in SA concentration down to the room temperature, which suggests that the copolymer micelles undergo dehydration in the presence of SA. SA is a weak acid with a pK_a value of 2.97 and has about 0.2% (0.0174 M) solubility in water at 30 °C.[60,61] Fig. 1a suggests that in the presence of P85, its solubility enhances quite significantly because of its solubilization within the P85 micelles. To obtain a rough estimate about the capacity of the P85 micelles to solubilize SA, we have also determined the concentrations of SA that cause phase separation at 30 °C as a function of P85 concentrations. A plot in Fig. 2 shows that as expected, the solubilization capacity of SA by P85 solution increases with increase in P85

concentration because of the increasing presence of P85 micelles. The concentration of P85 in this figure is expressed in moles per litre corresponding to 1%, 3%, 5% and 7% P85 solutions. To get the concentration of SA solubilized within the micelles we deducted the solubility of SA in water at 30 °C (0.0174 M)[61] from the total solubilization obtained. It is assumed that the solubility in water does not change with P85 concentration since the observed increase in solubilization with increase in P85 concentration shows almost a linear behavior. The plots of the obtained concentration of SA solubilized in the P85 micelles along with the corresponding number of moles of SA per mole of P85 are also shown in Fig. 2. It shows that the solubilization capacity of P85 micelles is about 8 molecules of SA per P85 molecules.

In order to understand the role of SA in bringing about the observed micellar dehydration, we have studied the effect of solubilization of SA on the fluorescence emission spectra of C153. The emission maximum of C153 is known to be sensitive to the polarity of its surrounding medium.[62] It undergoes blue shift with a decrease in the polarity of the medium, and a red shift with an increase in the same. Since in the case of Pluronics® this probe preferentially resides in the micellar corona region,[62] any change in the polarity of this region can be followed by studying its emission maximum. In the present case, the dehydration of the P85 micelles upon addition of SA is expected to lead to a blue shift of the emission maximum.[62] Contrary to that expectation, Fig. 3 shows that the emission maximum of C153 is red shifted upon addition of 0.1 M SA. A decrease in the polarity of the micellar corona region due to the loss of water is thus more than compensated by the presence of SA, which suggests that the SA molecules preferentially occupy the corona region of micelles. Since the dipole moment of SA is higher than that of water,[63] its presence in the corona as a substitute of water can lead to the observed increase in polarity of the micellar corona. Fig. 3 also shows the emission spectra for the P85 solution in the presence of 4 M NaCl. This salt is known to cause dehydration of the Pluronic® micelles due to the water structure making abilities of Na^+ and Cl^- ions. It can be seen from Fig. 3 that as expected, the emission maximum gets blue shifted in the presence of 4 M NaCl. The opposite behavior of these two cases, in spite of very similar effect on the CP, thus again suggests that SA molecules preferentially occupy the micellar corona region. This assumption agrees with the results of magnetic resonance spectroscopic studies on the solubilization of SA in the aqueous solution of
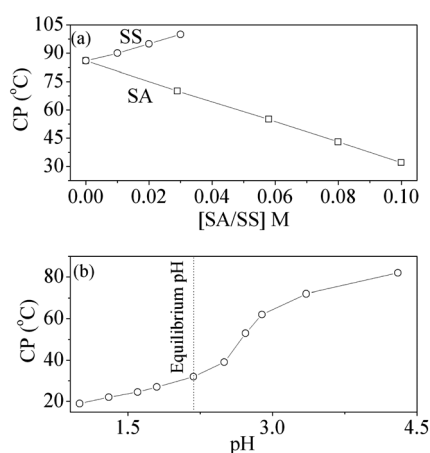

Fig. 1 Cloud point (CP) of the 5% P85 solution (a) as a function of salicylic acid (SA) and sodium salicylate (SS) concentrations and (b) as a function of pH in the presence of 0.1 M salicylic acid.
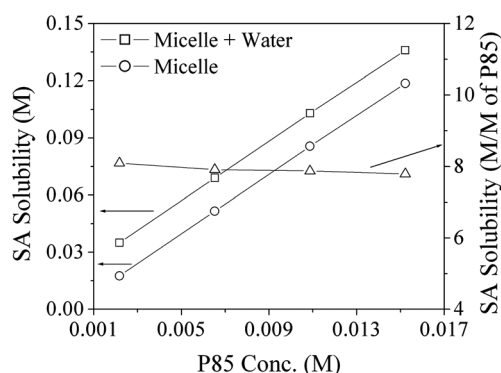

Fig. 2 Solubilization of salicylic acid (SA) at the cloud point (CP) of P85 solution as a function of P85 concentration.
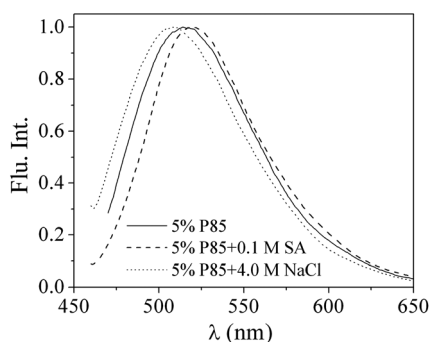
Fig. 3 Intensity normalized fluorescence spectra of C153 in 5% P85 solutions recorded at 30 °C.
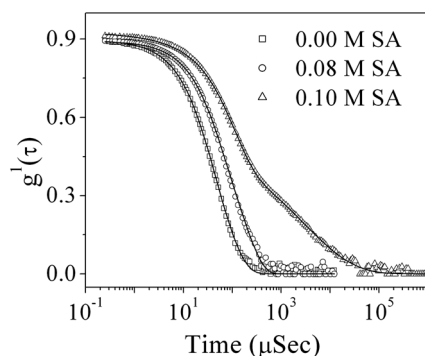

Fig. 4 Correlation function diagram of 5% P85 solution recorded at 30 °C and at 130° scattering angle as a function of salicylic acid concentration. The solid lines represent fit to the data.
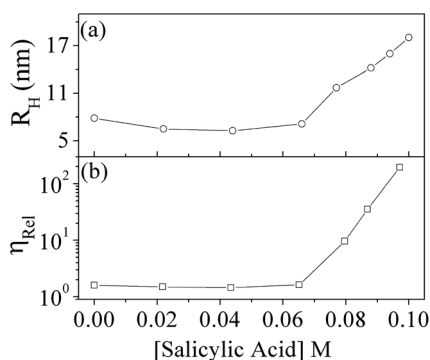

Fig. 5 (a) The hydrodynamic size of the P85 micelles as a function of salicylic acid concentration at 30 °C. (b) The relative viscosity of 5% P85 solution as a function of salicylic acid concentration at 30 °C.

alkyl ethoxylate type $[CH_3(CH_2)_{i-1}(OCH_2CH_2)_j{-}OH$ or $(C_iE_j)]$ nonionic surfactants.[64] These studies indicated that solubilized SA resides both in the micellar corona and in the core–corona interface through its interactions with the ethylene oxide, and the tendency of hydrocarbon blocks in the micellar core to solubilize the aromatic ring, respectively.[64]

To shed further light on the micellar dehydration by SA we studied the influence of sodium salicylate (SS) on 5% P85 solution and also that of pH on 5% P85 solution containing 0.1 M SA. The effect of SS has been studied to understand the influence
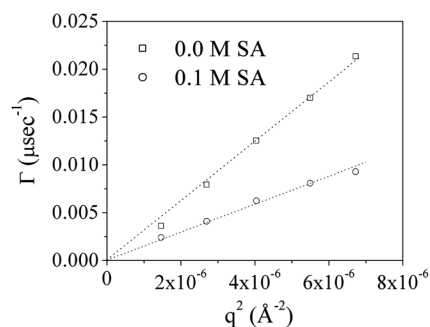

Fig. 6 The relaxation rate (Γ) vs. q^2 plots of 5% P85 solutions with 0.0 M and 0.1 M salicylic acid concentrations at 30 °C.
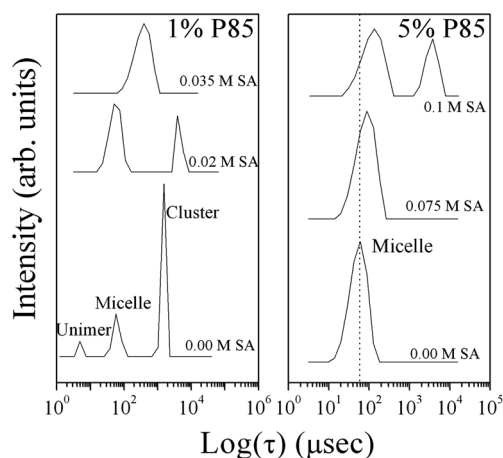

Fig. 7 Relaxation time distribution plots obtained from CONTIN analysis of the correlation function data of 1% P85 and 5% P85 solutions as a function of SA concentration.

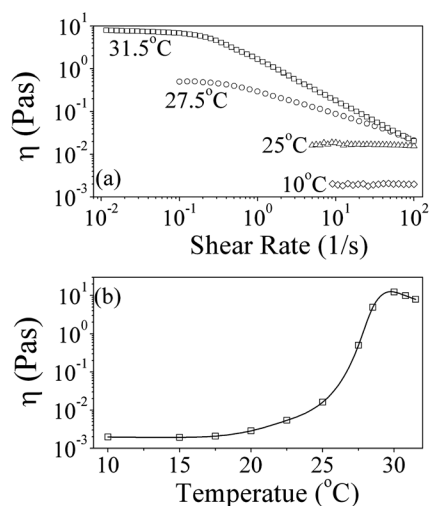**Fig. 8** (a) Viscosity of 5% P85 solution with 0.1 M salicylic acid as a function of shear rate at different temperatures. (b) Variation of zero shear viscosity of the same solution as a function of temperature.

of salicylate ions on the hydration properties of the copolymer micelles. The influence of pH, on the other hand, is studied to know whether it is the dissociated form or the un-dissociated
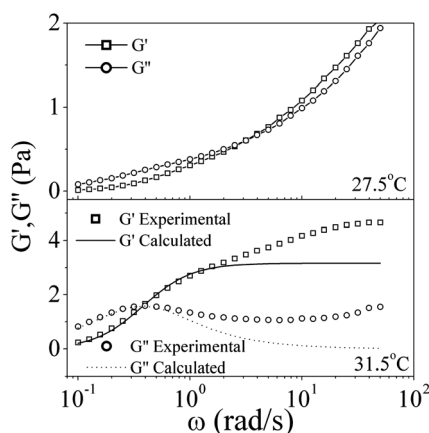
Fig. 9 Plots of storage modulus (G') and loss modulus (G'') of 5% P85 solution with 0.1 M salicylic acid as a function of frequency of the oscillatory shear at 27.5 °C and 31.5 °C.
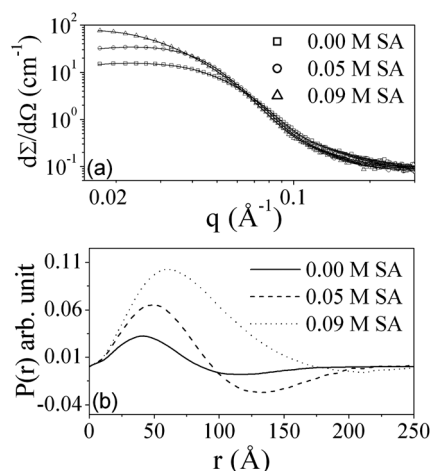

Fig. 10 (a) SANS patterns of 5% aqueous P85 solutions at 30 °C as a function of salicylic acid concentration. The solid lines represent the fit to the data using spherical and ellipsoidal form factors. (b) The corresponding pair distance distribution function [$P(r)$] plots as a function of salicylic acid concentration.

form of SA that causes dehydration of the P85 micelles. As shown in Fig. 1a, the addition of SS leads to an increase in the CP of the copolymer solution. This suggests that the observed dehydrating effect of SA on the P85 micelles does not arise due to the presence of salicylate ions generated by the dissociation of SA. This is also confirmed from the observed pH dependence of the CP of the copolymer solution containing 0.1 M SA. Fig. 1b shows that suppression of the dissociation of SA due to

a decrease in pH results in a decrease in the CP, which implies that interaction of the un-dissociated form of SA with the PEO blocks is responsible for the dehydration of the P85 micelles and the subsequent decrease in CP of the P85 solutions. The observed increase in CP with increases in SS concentration and pH could be attributed to the tendency of the salicylate ion to reside in the micellar corona region and subsequently impart ionic character in the micelles. The above-mentioned effects of SA and SS on the P85 micelles are different from those observed in the case of cetyltrimethyl ammonium bromide (CTAB) solutions, where both SA and SS bring about a sphere-to-rod growth of the CTAB micelles at comparable concentration ranges.[65–68] The obvious difference between these two cases is that unlike in the case of CTAB, it is not screening of charge but the dehydration of the P85 micelles in the presence of SA that leads to the micellar growth and shape change.

The P85 solutions are known to exhibit a sphere-to-rod micellar growth and a concomitant increase in viscosity on approaching their cloud points. To see whether the observed suppression of the CP in the presence of SA is accompanied by a simultaneous decrease in the sphere-to-rod shape transition temperature, we have studied the aggregation characteristics of the P85 as a function of SA using the DLS technique. The evolution of the correlation function diagram characteristic of these solutions as a function of SA concentration is shown in Fig. 4. A large shift in these diagrams with increase in SA concentration to higher time scale suggests that P85 micelles indeed undergo significant growth as the CP of the P85 solution approaches the room temperature (Fig. 1a). The observed shift in the correlation function diagram is also associated with a change in their nature from single exponential to bi-exponential. The analyses of the correlation function data were carried out based on the modified cumulant method at low SA concentration and the stretched bi-exponential equation when viscosity becomes high, as reported earlier in concentrated rod-like micellar systems.[69–71] The stretched bi-exponential equation is represented as

$$g^{(1)}(t) = A_f \exp(-t/\tau_f) + A_s \exp[-(t/\tau_s)^\beta] \quad (4)$$

where A_f and A_s are the amplitudes of the fast and slow relaxation modes corresponding to the relaxation time τ_f and τ_s, respectively.[69–71] The relaxation time for the fast mode is associated with the diffusion of the rod-like micelles and that of the slow mode can be ascribed to coupling between concentration fluctuation and stress relaxation in the entangled rod-like micelles. The exponent β ($0 < \beta \leq 1$) is inversely proportional to the width of the distribution of the relaxation times of the slow mode.[70]

Table 1 The core radius (R_c), the rod length (L), the hard sphere radius (R_{hs}), the aggregation number (N_{agg}), the volume fraction (ϕ) and the polydispersity ($\Delta R_c/R_{cm}$) of the micelles, and the radius of gyration of the PEO chain (R_g) in the micellar corona in 5% P85 solutions as a function of salicylic acid (SA) concentrations

[SA] mol l^{-1}	R_c (nm)	L (nm)	R_g (nm)	N_{agg}	R_{hs} (nm)	ϕ	$\Delta R_c/R_{cm}$ (%)
0.00	2.94 ± 0.02	—	0.9 ± 0.1	28 ± 1	6.82 ± 0.05	0.057 ± 0.003	27 ± 0.5
0.05	3.53 ± 0.03	—	1.5 ± 0.2	48 ± 1	7.73 ± 0.03	0.108 ± 0.006	29 ± 0.6
0.09	3.56 ± 0.03	15.6 ± 0.08	1.6 ± 0.2	215 ± 3	12.59 ± 0.04	0.087 ± 0.005	22 ± 0.6

The results of the analyses shown in Fig. 5a reveal that the size of the micelles increases sharply with increase in SA concentrations on the way to phase separation. These analyses also show that the relaxation rate (Γ) *vs.* q^2 plots for the micelles are linear both at low and high SA concentrations (Fig. 6). According to Ngai,[70] the relaxation rate of the slow mode is expected to show linear variation with $q^{2/\beta}$. We however did not observe any such linearity, which can be attributed to the possible presence of micellar clusters that could form near the CP and could contribute to the slow mode of the scattering pattern. Similar behavior was observed earlier in the aqueous Pluronic® system in the presence of salts that induce micellar dehydration and growth.[28]

To understand the nature of the growth of the P85 micelles induced by SA, we have also studied the viscosity of 5% P85 solution as a function of SA concentration. Fig. 5b shows that similar to what is observed in the case of the hydrodynamic size of the micelles (Fig. 5a), the relative viscosity of the P85 solution increases sharply with increase in SA concentration above 0.06 M (60 mM). The room temperature viscosities of Pluronic® solutions are determined primarily by the concentration and the shape of the Pluronic® micelles.[28,72] The observed increase in viscosity by about two orders of magnitude at a constant P85 concentration suggests that micellar growth is associated with a sphere-to-rod shape transition.[73]

To study the dependence of the observed salicylic acid induced micellar growth on P85 concentration, we have also carried out room temperature (30 °C) DLS studies on 1% P85 solution at different SA concentrations. Fig. 7 shows a comparison of the results of CONTIN analysis[74] of the correlation function data of 1% and 5% copolymer solutions as a function of SA concentration, carried out based on inverse Laplace transformation:

$$g^1(t) = \int_{-\alpha}^{\alpha} \tau A(\tau) e^{-t/\tau} d(\ln\tau) \qquad (5)$$

The corresponding plots of the correlation function data for 1% P85 solutions are shown in Fig. A of the ESI†. The CMT of the 1% P85 solution being close to the measurement temperature (29 °C),[8] the relaxation time distribution data of this solution show signatures of the presence of unimers, micelles and the micellar clusters.[11] Addition of SA is expected to increase the CMT of the copolymer solution due to its dehydrating effect on the copolymer molecules. This is reflected in the disappearance of first the unimers and then the micellar clusters with an increase in SA concentration, apart from a growth of the P85 micelles. The 5% P85 solution with lower CMT[8] than the 1% solution, on the other hand, does not show distinct features for the presence of either unimers or micellar clusters in the relaxation time distribution plot (Fig. 7). A broad relaxation time distribution of the micelles however suggests that albeit in smaller number, these species could be present in the solution at this copolymer concentration too. The micellar growth is reflected in increase in the relaxation time for the micelles, and at 0.1 M SA concentration the signature of the presence of coupling between concentration fluctuation and stress relaxation of the entangled rod-like micelles (mentioned earlier) is also seen at the high relaxation time zone. Such signature is absent at low concentration (1%) because of the absence of any entanglement of the rod like micelles.

Rheological studies

To understand more about the SA induced room temperature growth of P85 micelles, we have carried out rheological studies on 5% P85 solution with 0.1 M SA as a function of temperature on approaching the CP. An important feature of the rheology of worm like micellar systems is the deviation from the Newtonian behavior in the form of shear dependence of viscosity in the semi-dilute regime.[73] To see whether such behavior is also associated with the micellar growth in the present system, we studied the shear dependence of the viscosity of 5% P85 solution with 0.1 M SA as a function of temperature up to its CP (32 °C). Fig. 8a shows that as the micelles grow with increase in temperature, the viscosity of the P85 solution starts showing shear thinning. It arises due to the alignment of the worm like micelles along the direction of the shear induced flow and consequent breaking of their entangled network structure. The evolution of its zero shear viscosity as a function of temperature up to its cloud point is represented in Fig. 8b. As shown in the figure, the zero shear viscosity increases by about four orders of magnitude as the micelles undergo sphere-to-rod growth on approaching the CP. The observed decrease in the viscosity above 30 °C after a sharp increase can be attributed to branching of the micelles, which provides an additional mechanism for the stress relaxation as the branch points can slide along the length of the micelles.[75]

The viscoelastic behavior of the entangled micelles in a semi-dilute regime is analogous to that of living polymeric networks that often obey the simple Maxwell model. The dynamics of such a system has been studied in detail by Cates and Candau,[76,77] which involves two time scales namely the reptation time (τ_{rep}), and the breaking time (τ_b) of the micelles. The reptation time corresponds to the curvilinear diffusion of a chain along its own contour in a tube that is formed by the entangled neighboring chains. Both the reptation time and breaking time are a function of the length of the rod like micelles. An increase in length of the micelles results in an increase in the reptation time, but a decrease in the breaking time.[78] The ratio of these two relaxation times ($\zeta = \tau_b/\tau_{rep}$) controls the relaxation behavior of the worm like micelles.[77] For very small values of ζ, a single relaxation time dominates and Maxwell behavior is observed. For larger values of ζ on the other hand, existence of a spectrum of relaxation times leads to deviations from the Maxwell behavior, which is similar to that observed in the polymer solutions with wide molecular weight distributions.[78]

Rheological studies on the worm like micellar solutions of Pluronics® P84, P103, P105 and P123 show that they belong to the second category because of their slow micellar breaking processes.[79–82] It has also been shown that the P123 worm like micellar solutions obey the Maxwell law in the presence of 10–15% ethanol.[81] Ethanol increases the CMC and the CMT of the aqueous Pluronic® solutions as its interactions with the PPO and PEO groups reduce the overall hydrophobicity of the Pluronic® molecules.[32,33] The solvation of the micellar core in its presence also accelerates the dynamics of the aggregation characteristics of the Pluronic® micelles.[83–85] This is likely to be responsible for the observed rapid micellar breaking process and a consequent conformity with the Maxwell law in the P123 micellar solution in the presence of ethanol. The aggregation dynamics and hence the restructuring of the Pluronic® micelles

has also been found to be dependent on their molecular weight and hydrophobicity.[29,85,86] P85 is less hydrophobic than P84, P103, and P123 because of its higher hydrophilic PEO block content (50%). The breaking processes of worm like micelles are thus expected to be faster in the aqueous P85 solution as compared to that of these three copolymers. The dynamics of the aggregation characteristics of the Pluronic® micelles has also been shown to become faster with decrease in the molecular weight of the Pluronic® molecules.[85,86] The breaking process of the P85 ($M_w \approx 4200$ g mol^{-1}) micelles is thus expected to be faster than that of the P105 ($M_w \approx 6500$ g mol^{-1}) micelles too, though its hydrophobicity is comparable to that of P105.[85,86] To understand whether the above-mentioned differences of P85 with the other copolymers are reflected in the viscoelastic behavior of P85 solutions, we have studied the variation of G' and G'' as a function of frequency for 5% P85 solution with 0.1 M SA where the micelles grow with increase in temperature (Fig. 9). The figure shows typical viscoelastic behavior at 27.5 °C and 31.5 °C, as $G'(\omega)$ and $G''(\omega)$ cross each other at an intermediate frequency, i.e., the crossover frequency (ω_R). As expected, the crossover frequency decreases as the micelles grow with increase in temperature, but quite interestingly, the nature of the variation of G' and G'' too is found to be very different at these two temperatures. At 27.5 °C, when the micellar growth is incomplete, the observed variations are similar to those observed in other Pluronic® worm like micellar systems, with no sign of conformity with the Maxwell behavior in the low frequency region. At 31.5 °C, when the micelles have become bigger, the variations in G' and G'' on the other hand show compliance with the Maxwell behavior with a peak in G'' and a sharp increase in G' in the low frequency region. This can be attributed to a decrease in the breaking time (τ_b) and an increase in the reptation time (τ_{rep}) that leads to a decrease in ζ, as the length of the micelles increases with increase in temperature.[78,81] Assuming that at 31.5 °C the observed behavior of G' and G'' is close to that predicted by the Maxwell model, the relaxation time and plateau modulus can be obtained from the values of modulus and frequency at the crossover point. The stress relaxation time (τ_R) is obtained as the reciprocal of the crossover frequency (ω_R), while the plateau modulus can be taken as twice the value of the modulus at the crossover point.

As per the Maxwell model, the storage (G') and the loss (G'') moduli are defined as:

$$G'(\omega) = \frac{(\omega\tau_R)^2}{1 + (\omega\tau_R)^2} G_0 \qquad (6)$$

$$G''(\omega) = \frac{\omega\tau_R}{1 + (\omega\tau_R)^2} G_0 \qquad (7)$$

where G_0 is the plateau modulus and τ_R ($=\eta_0/G_0$) is the relaxation time. The calculated plots obtained using these equations with the τ_R and G_0 values generated from the experimental plots are also shown in Fig. 9. It can be seen that unlike in the case of other Pluronics®, there is reasonably good matching between the calculated and experimental plots in the low frequency region. The observed upturn of both G' and G'' at the higher frequencies can be attributed to the occurrence of fast relaxation processes such as breathing and Rouse relaxation modes. The breathing mode is associated with tube-length fluctuations, whereas the

Rouse mode refers to the local motions of the chain segments that are shorter than the entanglement length.[87]

The above rheological studies thus support the conjecture made from the DLS and viscometry studies that the SA induced growth of the P85 micelles is associated with a sphere-to-rod transition. The studies also suggest that the breaking and restructuring process of the P85 worm like micelles is faster than the worm like micelles of other Pluronics® due to the low molecular weight and large PEO content of P85.

Small angle neutron scattering studies

SANS studies on the SA induced growth of the P85 micelles are represented in Fig. 10. Fig. 10a shows the evolution of the SANS pattern with increase in the SA concentration at 30 °C. The plots containing the corresponding error bars are shown in Fig. B of the ESI†. It can be seen from Fig. 10 that the scattering intensity in the low q region increases quite significantly as the SA concentration increases from 0.00 M to 0.05 M (50 mM) and then to 0.09 M (90 mM). The data at 0.00 M and 0.05 M SA concentrations could be analyzed based on the spherical form factor, whereas the data at 0.09 M SA concentrations could only be fitted based on the ellipsoidal form factor. The results of the analysis of the data are shown in Table 1, which show that the aggregation number of the micelles increases as the micelles grow rod like. The micellar volume fraction, which includes water of hydration, first increases upon addition of 0.05 M SA but then decreases at 0.09 M SA concentration. The initial increase in the micellar volume fraction in spite of the dehydrating effect of SA can be attributed to the conversion of P85 unimers to micelles in the presence of SA. The observed decrease in the micellar volume fraction as the SA concentration increases from 0.05 M to 0.09 M arises due to the decrease in the degree of micellar hydration. The table shows that in spite of the decrease in the degree of micellar hydration, the hard sphere radius increases at a significantly faster rate than the cross-sectional radius when the micelles change their shape at 0.09 M SA concentration. This could be attributed to an increase in the effective volume of the inter-micellar interaction arising due to the rod like shape of the micelles.[28,88] To confirm the shape change of the micelles by SA, we also calculated the pair distance distribution functions [$p(r)$] from the SANS plots using the program GNOM made by Svergun and A. Semenyuk.[89,90] As shown in Fig. 10b, the asymmetry of the $p(r)$ plot increases significantly at 0.09 M SA concentration, which is a clear signature of an increase in the anisotropy of the micelles. These SANS studies thus corroborate the results of the DLS and rheological studies that the SA induced growth of the P85 micelles leads to sphere-to-rod shape transition. The rod like micelles thus formed are likely to be the equilibrium structure of the P85 micelles as it has been shown that the relaxation time associated with the dehydration induced restructuring of the P85 micelles is in the range of 10–100 milliseconds.[29,91]

Conclusion

In view of the potential applicability of Pluronics® as the solubilizing agent of the bio-medically important substances, we have studied the influence of solubilization of salicylic acid (SA) on the

aggregation characteristics of Pluronic® P85 in the aqueous medium. SA is an important drug for the treatment of various skin diseases and its entrapment in the micelles is an important issue in its applicability. Our aim thus has been to study the capacity of the biomedically relevant Pluronic® P85 to entrap SA and to modify the viscosity of the micellar solutions. Our DLS, viscometry, rheological and SANS studies show that the solubilization of SA in aqueous P85 solution leads to a sphere-to-rod micellar growth and a concomitant increase in the viscosity of the P85 solution. The observed micellar growth at the room temperature is attributed to the dehydrating effect of SA on the P85 micelles and a consequent decrease in the CP of the P85 solutions. Rheological studies suggest that unlike other aqueous Pluronic® systems, the present worm like micellar solutions show conformity with the Maxwell law, which could be attributed to the faster breaking process of the P85 micelles.

Acknowledgements

References

1 B. Chu, *Langmuir*, 1995, **11**, 414.
2 G. Wanka, H. Hoffmann and W. Ulbricht, *Macromolecules*, 1994, **27**, 4145.
3 P. N. Hurter and T. A. Hatton, *Langmuir*, 1992, **8**, 1291.
4 K. Zhang and A. Khan, *Macromolecules*, 1995, **28**, 3807.
5 S. Hvidt, E. B. Jorgensen, W. Brown and K. Schillen, *J. Phys. Chem.*, 1994, **98**, 12320.
6 K. Mortensen, W. Brown and B. Norden, *Phys. Rev. Lett.*, 1992, **68**, 2340.
7 M. Malmsten and B. Lindman, *Macromolecules*, 1992, **25**, 1282.
8 P. Alexandridis, J. F. Holzwarth and T. A. Hatton, *Macromolecules*, 1994, **27**, 2414.
9 G. Wanka, H. Hoffmann and W. Ulbricht, *Colloid Polym. Sci.*, 1990, **268**, 101.
10 O. Glatter, G. Scherf, K. Schillen and W. Brown, *Macromolecules*, 1994, **27**, 6046.
11 W. Brown, K. Schillen, M. Almgren, S. Hvidt and P. Bahadur, *J. Phys. Chem.*, 1991, **95**, 1850.
12 I. R. Schmolka, *J. Am. Oil Chem. Soc.*, 1977, **54**, 110.
13 N. K. Pandit and D. Wang, *Int. J. Pharm.*, 1998, **167**, 183.
14 G. A. Husseini, N. M. Abdel-Jabbar, F. S. Mjalli, W. G. Pitt and A. Al-Mousa, *J. Franklin Inst.*, 2011, **348**, 1276.
15 G. A. Husseini, N. M. Abdel-Jabbar, F. S. Mjalli and W. G. Pitt, *Technol. Cancer Res. Treat.*, 2007, **6**, 49.
16 G. A. Husseini, M. A. Diaz de la Rosa, E. O. AlAqqad, S. A. Mamary, Y. Kadimati, A. Al Baik and W. G. Pitt, *J. Franklin Inst.*, 2011, **348**, 125.
17 S. S. Kulthe, N. N. Inamdar, Y. M. Choudhari, S. M. Shirolikar, L. C. Borde and V. K. Mourya, *Colloids Surf., B*, 2011, **88**, 691.
18 W. I. Choi, J. H. Lee, J.-Y. Kim, J.-C. Kim, Y. H. Kim and G. Tae, *J. Controlled Release*, 2012, **157**, 272.
19 W. Zhang, Y. Shi, Y. Chen, J. Ye, X. Sha and X. Fang, *Biomaterials*, 2011, **32**, 2894.
20 W. Zhang, Y. Shi, Y. Chen, S. Yu, J. Hao, X. Sha and X. Fang, *Eur. J. Pharm. Biopharm.*, 2010, **75**, 341.
21 K. A. Witt, J. D. Huber, R. D. Egleton and T. P. Davis, *J. Pharmacol. Exp. Ther.*, 2002, **303**, 760.
22 T. C. Lai, K. Kataoka and G. S. Kwon, *Biomaterials*, 2011, **32**, 4594.
23 E. V. Batrakova, S. Li, Y. Li, V. Y. Alakhov, W. F. Elmquist and A. V. Kabanov, *J. Controlled Release*, 2004, **100**, 389.
24 A. A. Al-saden, T. L. Whateley and A. T. Florence, *J. Colloid Interface Sci.*, 1982, **90**, 303.
25 Z. Zhou and B. Chu, *J. Colloid Interface Sci.*, 1988, **126**, 171.
26 K. Mortensen and J. S. Pedersen, *Macromolecules*, 1993, **26**, 805.
27 W.-R. Chen, F. Mallamace, C. J. Glinka, E. Fratini and S.-H. Chen, *Phys. Rev. E: Stat., Nonlinear, Soft Matter Phys.*, 2003, **68**, 041402.
28 R. Ganguly, N. Choudhury, V. K. Aswal and P. A. Hassan, *J. Phys. Chem. B*, 2009, **113**, 668.
29 M. J. Kositza, C. Bohne, P. Alexandridis, T. A. Hatton and J. F. Holzwarth, *Macromolecules*, 1999, **32**, 5539.
30 P. Alexdandridis and J. F. Holzwarth, *Langmuir*, 1997, **13**, 6074.
31 R. Ganguly, V. K. Aswal, P. A. Hassan, I. K. Gopalakrishnan and J. V. Yakhmi, *J. Phys. Chem. B*, 2005, **109**, 5653.
32 J. Armstrong, B. Chowdhry, J. Mitchel, A. Beezer and S. Leharne, *J. Phys. Chem.*, 1996, **100**, 1738.
33 R. Ivanova, B. Lindman and P. Alexdandris, *Adv. Colloid Interface Sci.*, 2001, **89**, 351.
34 P. Holmqvist, P. Alexdandris and B. Lindman, *Langmuir*, 1997, **13**, 2471.
35 P. Holmqvist, P. Alexdandris and B. Lindman, *J. Phys. Chem. B*, 1998, **102**, 1149.
36 P. Holmqvist, P. Alexdandris and B. Lindman, *Macromolecules*, 1997, **30**, 6788.
37 L. Guo, R. H. Colby and P. Thiyagarajan, *Physica B*, 2006, **385**, 685.
38 Y. L. Su, X. F. Wei and H. Z. Liu, *Langmuir*, 2003, **19**, 2995.
39 A. Caragheorgheopol, H. Caldararu, I. Dragutan, H. Joela and W. Brown, *Langmuir*, 1997, **13**, 6912.
40 J. H. Ma, Y. Wang, C. Guo and H. Z. Liu, *J. Phys. Chem. B*, 2007, **111**, 11140.
41 J. P. Mata, P. R. Majhi, O. Kubota, A. Khanal, K. Nakashima and P. Bahadur, *J. Colloid Interface Sci.*, 2008, **320**, 275.
42 L. Heerema, D. Cakali, M. Roelands, E. Goetheer, D. Verdoes and J. Keurentjes, *Sep. Purif. Technol.*, 2010, **74**, 55.
43 L. Rhein, B. Chaudruri, N. Jivani, H. Fares and A. Davis, *J. Cosmet. Sci.*, 2004, **55**, 65.
44 E. R. Cooper, *J. Pharm. Sci.*, 1984, **73**, 1153.
45 P. Singh and M. S. Roberts, *J. Pharmacol. Exp. Ther.*, 1994, **268**, 144.
46 M. Davies and R. Marks, *Br. J. Dermatol.*, 1976, **95**, 187.
47 E. Weirich, *Dermatologica*, 1975, **151**, 268.
48 J.-C. Tsai, S.-A. Chuang, M.-Y. Hsu and H.-M. Sheu, *Int. J. Pharm.*, 1999, **188**, 145.
49 S. E. Cross, R. Jiang, H. A. E. Benson and M. S. Roberts, *J. Invest. Dermatol.*, 2001, **117**, 147.
50 I. R. Schmolka, *J. Biomed. Mater. Res.*, 1972, **6**, 571.
51 P. A. Hassan and S. K. Kulshreshtha, *J. Colloid Interface Sci.*, 2006, **300**, 744.
52 D. E. Koppel, *J. Chem. Phys.*, 1972, **57**, 4814.
53 ASTM Standard D 445-04 and D 446-04 2004, and the references within.
54 V. K. Aswal and P. S. Goyel, *Curr. Sci.*, 2000, **79**, 947.
55 J. S. Pedersen and C. Gerstenberg, *Macromolecules*, 1996, **29**, 1363.
56 J. S. Pedersen, *J. Appl. Crystallogr.*, 2000, **33**, 637.
57 J. S. Pedersen and C. Gerstenberg, *Macromolecules*, 1996, **29**, 1363.
58 J. K. Percus and G. J. Yevick, *Phys. Rev.*, 1958, **1**, 110.
59 J. S. Pedersen, *Adv. Colloid Interface Sci.*, 1997, **70**, 171.
60 A. Shalmashi and A. Eliassi, *J. Chem. Eng. Data*, 2008, **53**, 199.
61 J. M. P. Q. Delgado, *Heat Mass Transfer*, 2007, **43**, 1311.
62 M. Kumbhakar, *J. Phys. Chem. B*, 2007, **111**, 14250.
63 M. Da Silva, C. M. S. Menezes, E. I. Ferreira, C. Q. F. Leite, D. N. Sato, C. C. Correia, C. P. Pimenta and K. C. A. Botelho, *Chem. Biol. Drug Des.*, 2008, **71**, 167.
64 M. Donbrow, P. Molyneux and C. T. Rhodes, *J. Chem. Soc. A*, 1967, 561.
65 T. Shikata, H. Hirata and T. Kotaka, *J. Phys. Chem.*, 1990, **94**, 3702.
66 T. Shikata, Y. Sakaiguchi, H. Uragami, A. Tamura and H. Hirata, *J. Colloid Interface Sci.*, 1987, **119**, 291.
67 T. A. Strivens, *Colloid Polym. Sci.*, 1989, **267**, 269.
68 T. Shikata, H. Hirata and T. Kotaka, *Langmuir*, 1989, **5**, 398.
69 C. Moitzi, N. Freiberger and O. Glatter, *J. Phys. Chem. B*, 2005, **109**, 16161.
70 K. L. Ngai, *Adv. Colloid Interface Sci.*, 1996, **64**, 1.
71 R. Ganguly, V. K. Aswal and P. A. Hassan, *J. Colloid Interface Sci.*, 2007, **315**, 693.
72 R. Ganguly, V. K. Aswal, P. A. Hassan, I. K. Gopalakrishnan and S. K. Kulshreshtha, *J. Phys. Chem. B*, 2006, **110**, 9843.
73 D. Löf, K. Schillén, M. F. Torres and A. J. Müller, *Langmuir*, 2007, **23**, 11000.
74 S. W. Provencher, *Comput. Phys. Commun.*, 1982, **27**, 229.

75 P. Koshy, V. K. Aswal, M. Venkatesh and P. A. Hassan, *J. Phys. Chem. B*, 2011, **115**, 10817.
76 M. E. Cates, *J. Phys. Chem. B*, 1990, **94**, 371.
77 M. E. Cates and S. J. Candau, *J. Phys.: Condens. Matter*, 1990, **2**, 6869.
78 M. E. Cates, *Macromolecules*, 1987, **20**, 2289.
79 G. Waton, B. Michels, A. Steyer and F. Schosseler, *Macromolecules*, 2004, **37**, 2313.
80 V. Castelletto, P. Parras, I. W. Hamley, P. Bäverbäck, J. S. Pedersen and P. Panine, *Langmuir*, 2007, **23**, 6896.
81 A. G. Denkova, E. Mendes and M.-O. Coppens, *J. Rheol.*, 2009, **53**, 1087.
82 V. V. A. Fernández, N. Tepale, J. G. Álvarez, J. H. Pérez-López, E. R. Macías, F. Bautista, F. Pignon, Y. Rharbi, R. Gámez-Corrales, O. Manero, J. E. Puig and J. F. E. Soltero, *J. Colloid Interface Sci.*, 2009, **336**, 842.

83 S. S. Soni, G. Brotons, M. Bellour, T. Narayanan and A. Gibaud, *J. Phys. Chem. B*, 2006, **110**, 15157.
84 A. G. Denkova, E. Mendes and M.-O. Coppens, *J. Phys. Chem. B*, 2009, **113**, 989.
85 Y. Kadam, R. Ganguly, M. Kumbhakar, V. K. Aswal, P. A. Hassan and P. Bahadur, *J. Phys. Chem. B*, 2009, **113**, 16296.
86 M. J. Kositza, C. Bohne, P. Alexandridis, T. A. Hatton and J. F. Holzwarth, *Langmuir*, 1999, **15**, 322.
87 R. Granek and M. E. Cates, *J. Chem. Phys.*, 1992, **96**, 4758.
88 R. Ganguly, M. Kumbhakar and V. K. Aswal, *J. Phys. Chem. B*, 2009, **113**, 9441.
89 D. I. Svergun, A. V. Semenyuk and L. A. Feigin, *Acta Crystallogr., Sect. A: Found. Crystallogr.*, 1988, **44**, 244–251.
90 D. I. Svergun, *J. Appl. Crystallogr.*, 1991, **24**, 485–492.
91 I. Goldmints, J. F. Holzwarth, K. A. Smith and T. A. Hatton, *Langmuir*, 1997, **13**, 6130.